Target fragments from the interaction of ^{93}Nb and ^{181}Ta with 47 MeV/nucleon ^{12}C ions

Li Wenxin and Sun Tongyu
Institute of Modern Physics, Academia Sinica, Lanzhou, 730000, China

Chih Tahai
China Institute of Atomic Energy, Beijing, 102413, China

Li Yunsheng
Institute of Modern Physics, Academia Sinica, Lanzhou, 730000, China

Zheng Yuming
China Institute of Atomic Energy, Beijing, 102413, China
and Chinese Center of Advanced Science and Technology (World Laboratory), Beijing, China

Sun Ruling, Zhao Lili, Wu Dingqing, and Jing Genming
Institute of Modern Physics, Academia Sinica, Lanzhou, 730000, China

Sa Benhao
China Institute of Atomic Energy, Beijing, 102413, China
and Chinese Center of Advanced Science and Technology (World Laboratory), Beijing, China
(Received 15 January 1993)

Cross sections for the production of the target fragments in the interaction of ^{93}Nb and ^{181}Ta with 47 MeV/nucleon ^{12}C ions have been measured with off-line γ spectroscopy. The mass yield distributions were deduced assuming a Gaussian charge distribution function. The results were compared with statistical fusion-fragmentation model calculations.

PACS number(s): 24.60.$-$k, 25.70.Mn

I. INTRODUCTION

The mass yield distribution of the target fragments is one of the most important characteristics of a nuclear reaction induced by energetic heavy ions. At present a large amount of information on the mass yield distributions has been cumulated. However, theoretical explanations of the experimental mass distribution in intermediate-energy heavy-ion reactions are not always successful. For example, neither cascade-evaporation calculations using Monte Carlo techniques [1] nor incomplete fusion model calculations using the preequilibrium codes ALICE and EVA could [2] give satisfactory agreement with the mass distributions measured in the reactions of ^{nat}Cu with 86- and 35-MeV/nucleon ^{12}C ions. Recently a statistical fusion-fragmentation model describing the disassembly of hot nuclei created in intermediate-energy heavy-ion collisions has been developed and it successfully reproduced the experimental mass yield distributions for the reactions of ^{nat}Cu with 35- [3] and 44-MeV/nucleon [4] ^{12}C ions. In this work we present the mass yield distributions of the target fragments from the interaction of ^{93}Nb and ^{181}Ta with 47-MeV/nucleon ^{12}C ions. The experimental results were compared with calculations based on the statistical fusion-fragmentation model with the purpose of extending the range of validity of this model. Preliminary results have been reported elsewhere [5,6].

II. EXPERIMENT

The irradiations were performed with 47-MeV/nucleon ^{12}C ions delivered from the Heavy Ion Research Facility (HIRFL) at the Institute of Modern Physics, Lanzhou, Academia Sinica. The targets used for the irradiation consisted of 99.9% pure natural niobium and tantalum foils with thickness of 41.6 and 102 mg/cm^2, respectively. Each target was surrounded by two Mylar foils used as forward and backward recoil catcher foils. Additional Mylar foils served as activation blanks and the whole target assembly was surrounded by another two Mylar foils which served to guard the assembly from possible external sources of radioactive products. All the Mylar foils have a thickness of 10.5 mg/cm^2.

The target stacks were mounted in an evacuated chamber terminated with a Faraday cup. A bias voltage of -100 V was imposed on a biasing ring of the Faraday cup to suppress escape of electrons. Two separate bombardments were done, 10 h in duration for each, with typical intensities of 5–10 electrical nA. The energies at the center of the targets were reduced from 47 to 46 MeV/nucleon and 45 MeV/nucleon for ^{93}Nb and ^{181}Ta targets, respectively, owing to the energy loss in Mylar and target foils [7]. The beam intensity was recorded at periodic intervals by a current integrator. The fluences were 745 μC or 7.8×10^{14} ^{12}C ions and 211 μC or 2.2×10^{14} ^{12}C ions for the niobium and tantalum runs, respectively.

Following irradiation, the targets and forward and backward catcher foils were assayed with a calibrated HGe γ-ray spectrometer. The detector has 40% efficiency and 2.2 keV resolution at 1.332 MeV. The measurement of γ rays began about 30 min after the end of irradiation and lasted for 2 months.

The γ-ray spectra recorded on 4096 channels were analyzed with the code SAMPO [8]. The decay curves were analyzed with an iterative code run on the graphics terminal Tektronix-4014. The identification of the activities present in each foil and the calculation of cross sections from these activities were very similar to those described in Ref. [9]. Nuclear data used for the cross-section calcu-

TABLE I. Cross sections (in mb) observed in this work.

Nuclide	^{12}C±^{93}Nb	^{12}C±^{181}Ta	Nuclide	^{12}C±^{93}Nb	^{12}C±^{181}Ta
^{22}Na	3.18±1.2	2.8±1.3	^{92}Nb *m* (I)	62.5±5.5	
^{24}Na	1.23±0.12	2.1±0.3	^{93}Mo *m*	11.4±1.6	2.4±0.2
^{44}Sc *m* (I)		1.2±0.7	^{94}Tc *g*	1.06±0.19	4.4±0.2
^{46}Sc *g* (I)	0.78±0.08		^{95}Tc *m*		3.8±1.0
^{48}Sc (I)	0.087±0.04	1.7±0.2	^{95}Tc *g*		9.2±1.0
^{48}V	0.79±0.07	0.46±0.07	^{95}Zr		1.1±0.1
^{51}Cr	1.89±0.24		^{97}Ru		7.3±2.0
^{52}Mn *g*	0.66±0.07		^{99}Mo		2.6±0.4
^{54}Mn (I)		3.3±0.5	^{100}Rh		2.8±0.3
^{55}Co	5.92±0.73		^{101}Rh *m*		1.4±0.3
^{56}Co	0.80±0.07		^{103}Ru		3.9±1.3
^{57}Ni		3.6±1.3	^{105}Ag *g*		5.3±1.3
^{58}Co	4.76±0.49	6.4±0.6	^{105}Rh *g*		2.9±0.4
^{59}Fe	0.34±0.07	4.1±0.3	^{106}Ag *m*		2.9±0.2
^{62}Zn	0.56±0.27		^{110}In		2.1±0.2
^{65}Zn	18.0±2.3	3.9±0.5	^{111}In		5.1±0.5
^{66}Ga	8.45±1.2		^{119}Te		0.8±0.3
^{67}Ga	19.0±1.7	5.8±1.0	^{121}Te		3.3±0.9
^{68}Ge	19.2±4.9		^{124}Sb *g*		1.6±0.8
^{69}Ge	27.5±2.0	3.9±0.4	^{126}Sb *g*		1.8±0.5
^{70}As	21.6±4.8		^{128}Ba		3.3±0.2
^{71}As	32.7±2.3		^{129}Cs		4.7±1.2
^{72}Ga		4.8±0.8	^{131}Ba		4.5±1.6
^{72}Se	13.5±1.4		^{139}Ce		3.4±0.8
^{73}Se *g*	25.4±2.7		^{145}Eu		9.4±0.9
^{74}As (I)	10.8±0.7	9.8±0.9	^{146}Eu		11.4±1.1
^{75}Se	87.8±3.9	9.3±0.7	^{146}Gd		15.3±0.8
^{76}As	98.8±8.4		^{147}Gd		13.8±1.4
^{76}Br		8.3±3.3	^{148}Eu		11.6±2.8
^{76}Kr	8.3±0.9		^{153}Gd		53.5±4.0
^{77}Br	71.7±2.9		^{155}Dy		37.7±2.4
^{77}Kr	20.6±10.1		^{156}Tb		53.0±7.0
^{79}Kr	72.7±4.4		^{156}Ho		45.3±6.6
^{80}Sr	4.45±1.22		^{158}Er		72.1±6.3
^{81}Rb *g*	79.1±8.6		^{159}Er		74.8±7.9
^{82}Br (I)	9.53±1.49	5.7±0.8	^{160}Er		101±5
^{82}Rb *m* (I)	37.8±2.4		^{163}Tm		123±21
^{82}Sr	78.7±6.9		^{165}Tm		120±5
^{83}Rb	152.9±9.3	16.6±1.0	^{166}Yb		135±14
^{84}Rb *g* (I)	8.79±0.99	11.4±0.9	^{167}Tm		145±15
^{84}Y *g*	35.8±6.9		^{169}Yb		155±16
^{85}Sr	166±18	14.8±2.0	^{170}Hf		128±13
^{85}Y	51.9±5.3		^{172}Hf		136±14
^{86}Y *g*		5.5±0.5	^{175}Hf		103±10
^{86}Zr	41.0±4.3		^{175}Ta		132±13
^{88}Zr	137±14	6.7±1.5	^{176}W		247±25
^{89}Zr	156±14	9.1±1.0	^{177}Ta		179±20
^{89}Nb	84.6±21.8		^{178}W		90±9
^{90}Nb	129±8	7.9±1.2	^{181}Hf		19.8±7.2
^{90}Mo	14.8±1.2		^{182}Ta		10.7±1.0
^{91}Sr	13.4±3.3				

lation were quoted from Ref. [10]. The production cross sections of the nuclides were obtained on the basis of the total activities found in the target and catcher foils.

III. RESULTS

In the reactions of ^{93}Nb and ^{181}Ta induced by 47-MeV/nucleon ^{12}C ions, the production cross sections were determined for 35 and 81 target fragments, respectively. The data are summarized in Table I. The uncertainties listed in Table I are standard deviation, including errors in the analysis of the γ spectra and in the resolution of the decay curves by the least-squares method, and a 5% error in detector efficiencies. While the uncertainty in the thickness of the targets was negligible, the uncertainty in beam current measurement was not taken into account.

Although a large number of cross sections have been determined, the data represent only a fraction of the total isobaric yields. In order to obtain the mass yield distribution, it is necessary to make an estimation of the cross sections for unmeasured products. Thus, we have made an assumption of Gaussian charge distribution, that is, the independent yield cross section for a given species, $\sigma(Z,A)$, can be represented by a histogram that lies along a Gaussian curve:

$$\sigma(Z,A)=\sigma(A)\frac{1}{[2\pi C_Z^2(A)]^{1/2}}\exp\left\{-\frac{[Z-Z_P(A)]^2}{2C_Z^2(A)}\right\}, \quad (1)$$

where $\sigma(A)$ is the total isobaric yield, $C_Z(A)$ is the Gaussian width parameter for mass number A, and $Z_P(A)$ is the most probable Z value for that isobar, and can be written as a function of A,

$$Z_P(A)=K_0+K_1A+K_2A^2 . \quad (2)$$

Adjusting K_0, K_1, K_2, and the width parameter $C_Z(A)$, the fractional independent yields calculated were used to determine the Gaussian charge distributions by means of an iterative computer code. As a result the mass yield distributions were obtained from integrating the charge distributions and are shown in Figs. 1 and 2 for the interaction of ^{93}Nb and ^{181}Ta with 47-MeV/nucleon ^{12}C ions, respectively. The error bars shown in these figures reflect only the experimental uncertainties mentioned above, and do not take into account the uncertainty introduced from the charge distribution fitting process. The latter uncertainty may reach about 25%. Details, by which the mass yield distributions were constructed, have been described in our previous work [11].

As seen from Fig. 1, the mass distribution for 46-MeV/nucleon ^{12}C-ion-induced reaction of ^{93}Nb has a similar overall shape to that of ^{12}C+^{nat}Cu reaction [4,12]. The average mass number for this distribution is at $A=81$, 12 units below the target mass. The mass distribution for 45-MeV/nucleon ^{12}C-ion-induced reaction of ^{181}Ta shows approximately a form similar to one reported in the 545-MeV ^{12}C+^{197}Au reaction [13]. As seen from Fig. 2, there is a large hump consisting of the heavy target residues at the mass number slightly below the target mass. In addition to this hump, one can find a wide distribution at mass range of $A=50-110$. The centroid of this distribution is around $A=80$, suggesting that these products may result from binary fission of the targetlike species.

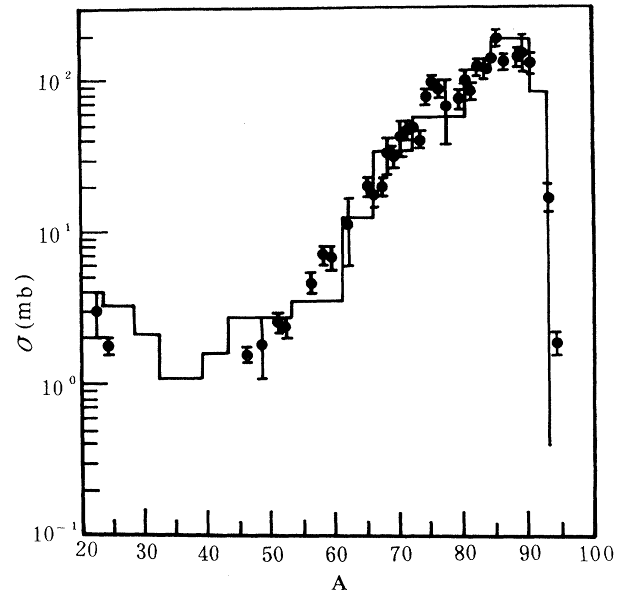

FIG. 1. Mass yield distribution for the interaction of niobium with 46-MeV/nucleon ^{12}C ions. The histograms represent statistical model calculations.

IV. DISCUSSION

A recently proposed statistical fusion-fragmentation model describing the disassembly of hot nuclei was used to calculate the mass yield distributions of the target resi-

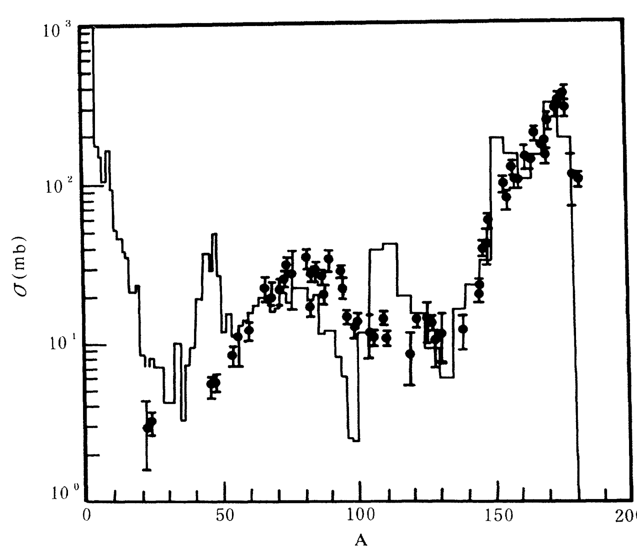

FIG. 2. The same as Fig. 1, except the interaction is tantalum with 45-MeV/nucleon ^{12}C ions.

dues measured in this work. The details of that model can be found in Refs. [3,14]. The basic features of the model are the following.

(1) As a product of initial interaction (incomplete fusion) of the intermediate-energy nucleus-nucleus collision, a composite nucleus is created. It consists of the target and a transferred projectile piece. This piece is composed of projectile nucleons located in the overlap region between the target nucleus and the projectile, with a given impact parameter, which is sampled with equal geometric probability [3].

(2) After heating and compression, the composite nucleus (hot nucleus) expands homogeneously towards a freeze-out state, where the hot nucleus is pictured as a sphere with the nucleon radius parameter r_h larger than the normal nucleon radius $r_0 = 1.15$ fm. The excitation energy of the hot nucleus at freeze-out is a fraction of available reaction energy described by another model parameter C_f [3] as

$$E_h^* = C_f E \ , \tag{3}$$

where the available reaction energy E is calculated on the basis of the reaction kinetics and mass balance [3] and on the assumption of that the missing mass in the initial interaction escapes as a whole cluster with beam velocity [15].

(3) The hot nucleus disassembles promptly into a configuration described by a set of variables $\{N_c, N_n, \{A_i, Z_i\}_{i=1}^{N_c}, \{\mathbf{r}_i\}_1^{N_c}, \{\mathbf{p}_i\}_1^{N_c}, \{\varepsilon_i\}_1^{N_c}, \{\mathbf{r}_j\}_1^{N_n}, \{\mathbf{p}_j\}_1^{N_n}\}$. Here N_c and N_n are the number of charged fragments including prompt protons and of prompt and evaporated neutrons, respectively. $\{A_i, Z_i\}_1^{N_c}, \{\mathbf{r}_i\}_1^{N_c}$, $\{\mathbf{p}_i\}_1^{N_c}$, and $\{\varepsilon_i\}_1^{N_c}$ are the set of mass and charge numbers, position, momentum, and internal excitation energy of charged fragments. $\{\mathbf{r}_j\}_1^{N_n}$ and $\{\mathbf{p}_j\}_1^{N_n}$ are the set of position and momentum of neutrons, respectively.

(4) The total energy of the hot nucleus at freeze-out is given by

$$E = E_{B,h} + E_h^* = E_B + E_c + E_{in}^* + E_{kf} + E_{kn} \ , \tag{4}$$

where

$$E_c = \sum_{i<j}^{N_c} \frac{Z_i Z_j e^2}{|\mathbf{r}_i - \mathbf{r}_j|} \ , \tag{5}$$

$$E_B = \sum_{i=1}^{N_c} E_{Bi} \ , \tag{6}$$

$$E_{in}^* = \sum_{i=1}^{N_c} \varepsilon_i \ , \tag{7}$$

$$E_{kf} = \sum_{i=1}^{N_c} P_i^2/2m_i \ , \tag{8}$$

and

$$E_{kn} = \sum_{j=1}^{N_n} P_j^2/2m_0 \tag{9}$$

are the Coulomb energy among fragments, the binding energy, the internal excitation energy, the kinetic energy of fragments, and the kinetic energy of neutrons, respectively. $E_{B,h}$ and E_h^* are the binding energy and excitation energy of the hot nucleus.

(5) The configurations allowed by mass, charge, momentum, and energy conservation are assumed to conform to a distribution of canonical [16] or microcanonical [17] ensembles. By means of Monte Carlo simulations and a corresponding Metropolis simulation, a large number of allowed configurations (10^6, for example) are generated. The physical observables are then calculated as a statistical average. Finally, an average over impact parameters is taken.

On this basis, theoretical calculations were performed for the reactions under study. The calculated results are shown, as histograms, in Figs. 1 and 2, respectively. As shown in Fig. 1, the theoretical results agree quite well with the experimental mass yield distribution for the reaction of 46-MeV/nucleon ^{12}C on ^{93}Nb. Some features, e.g., the peak position, the width of the distribution, and the upturn of the mass yield at $A < 30$, have been nicely reproduced by the calculations. Good agreement between the theoretical and the experimental mass distributions implies that the disassembly of hot nuclei is responsible for the production of the target fragments and all of the possible decay modes of the hot nuclei, i.e., pseudoevaporation mode, pseudofission mode, multifragmentation mode, and vaporization mode [3], and the competition among them are properly included in the statistical model.

For 45-MeV/nucleon ^{12}C$+^{181}$Ta reaction, the agreement between the calculated and measured mass yield distributions seems to be fairly satisfactory, especially for the heavy target fragments (see Fig. 2). The model is also able to roughly reproduce the yield distribution for the fission fragment, although centroid of the calculated yield distribution is shifted by almost ten mass units to the low mass side. However, large discrepancies between the measured and calculated distributions appear at mass regions of around $A = 45$ and $A = 110$. Theoretical results seem to indicate that the hot nucleus formed in the reaction of ^{12}C$+^{181}$Ta prefers an asymmetric pseudofission mode more than a symmetric one.

V. SUMMARY

The cross sections of the target fragments have been determined by the radiochemistry techniques for the interaction of ^{93}Nb and ^{181}Ta with 47-MeV/nucleon ^{12}C ions. Assuming a charge distribution, the mass yield distributions have been deduced. The experimental mass distributions were compared with a fusion-fragmentation model describing the disassembly of hot nuclei arising from intermediate-energy nucleus-nucleus collisions. Good agreement has been obtained for the reaction with nonfissionable ^{93}Nb target nucleus. A discrepancy between theoretical results and experimental mass distribution appears, however, in the fission product region for the reaction on the ^{181}Ta target nucleus. This is an open question and worthy of further study.

ACKNOWLEDGMENTS

We wish to thank Diana Lee of LBL for her assistance in computer codes and Professor W. Loveland of Oregon State University for his advice and correction for the manuscript of this paper. We appreciate the great effort of the accelerator personnel who made the first experiments at HIRFL possible. This work was supported, in part, by the National Natural Science Foundation of China.

---

[1] T. Lund, D. Molzahn, R. Brandt, B. Bergersen, D.Eriksen, E. Hagebo, I. R. Haldorsen, T. Bjornstad, and C. Richard-Serre, Phys. Lett. **102B**, 239 (1981).

[2] S. Y. Cho, Y. H. Chung, N. T. Porile, and D. J. Morrissey, Phys. Rev. C **36**, 2349 (1987).

[3] Sa Ben-Hao, Zhen Yu-Ming, and Zhang Xiao-Ze, Phys. Rev. C **40**, 2680 (1989).

[4] Li Wenxin, High Energy Phys. Nucl. Phys. **14**, 417 (1990).

[5] Li Wenxin, in *Proceedings of the Second IN2P3–RIKEN Symposium on Heavy-Ion Collisions,* Obernai, France, edited by B. Heusch (World Scientific, Singapore, 1991), p. 363.

[6] Li Wenxin, Sun Tongyu, Wu Dingqing, Sun Rulin, Zhao Lili, Jing Genming, Zheng Yuming, Chin Tahai, and Sa Benhao, in *Proceedings of the International Symposium on Heavy Ion Physics,* Lanzhou, China, 1990, edited by W. Q. Shen, Y. X. Luo, and J. Y. Liu (World Scientific, Singapore, 1991), p. 158.

[7] F. Hubert, A. Fleury, R. Bimbot, and D. Gardes, Ann. Phys. (Paris) **5**, 1 (1980).

[8] J. T. Routti and S. G. Prussin, Nucl. Instrum. Methods **72**, 125 (1969).

[9] D. J. Morrissey, D. Lee, R. J. Otto, and G. T. Seaborg, Nucl. Instrum. Methods **158**, 499 (1978).

[10] U. Reus and W. Westmeier, At. Data Nucl. Data Tables **29**, 2 (1983).

[11] Li Wenxin, Yin Xinmin, Luo Qingzheng, Zhao Lili, Sun Tongyu, and Wu Dingqing, Phys. Rev. C **46**, 1538 (1992).

[12] S. Y. Cho, N. T. Porile, and D. J. Morrissey, Phys. Rev. C **39**, 2227 (1989).

[13] W. Loveland, K. Aleklett, P. P. McGaughey, K. J. Moody, R. M. McFarland, R. H. Kraus, Jr., and G. T. Seaborg, LBL Report No. LBL-16870, 1984, p. 142.

[14] Chih Ta-Hai, Sa Ben-Hao, Zhang Xiao-Ze, and Zheng Yu-Ming, Phys. Rev. C **42**, 2187 (1990).

[15] S. Leary, J. Phys. C **4**, 175 (1986).

[16] Sa Ben-Hao and D. H. E. Gross, Nucl. Phys. **A437**, 643 (1985); Zhang Xiao-Ze, D. H. E. Gross, Xu Shu-Yan, and Zheng Yu-Ming, *ibid.* **A461**, 641 (1987).

[17] Zhang Xiao-Ze, D. H. E. Gross, Xu Shu-Yan, and Zheng Yu-Ming, Nucl. Phys. **A461**, 668 (1987).